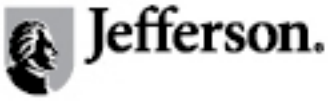

2-15-2012

Loss of αT-catenin alters the hybrid adhering junctions in the heart and leads to dilated cardiomyopathy and ventricular arrhythmia following acute ischemia.

Jifen Li
Center for Translational Medicine, Department of Medicine, Thomas Jefferson University, Jifen.Li@jefferson.edu

Steven Goossens
Department for Molecular Biomedical Research, Flanders Institute for Biotechnology (VIB); Department of Biomedical Molecular Biology, Ghent University

Jolanda van Hengel
Department for Molecular Biomedical Research, Flanders Institute for Biotechnology (VIB); Department of Biomedical Molecular Biology, Ghent University

Erhe Gao
Center for Translational Medicine, Department of Medicine, Thomas Jefferson University, Erhe.Gao@jefferson.edu

Lan Cheng
Center for Translational Medicine, Department of Medicine, Thomas Jefferson University, Lan.Cheng@jefferson.edu

See next page for additional authors

Authors
Jifen Li, Steven Goossens, Jolanda van Hengel, Erhe Gao, Lan Cheng, Koen Tyberghein, Xiying Shang, Riet De Rycke, Frans van Roy, and Glenn L Radice

Loss of αT-catenin alters the hybrid adhering junctions in the heart and leads to dilated cardiomyopathy and ventricular arrhythmia following acute ischemia

Jifen Li[1,*], Steven Goossens[2,3,‡], Jolanda van Hengel[2,3,‡], Erhe Gao[1], Lan Cheng[1], Koen Tyberghein[2,3], Xiying Shang[1], Riet De Rycke[2], Frans van Roy[2,3,*] and Glenn L. Radice[1]

[1]Center for Translational Medicine, Department of Medicine, Thomas Jefferson University, Philadelphia, PA, USA
[2]Department for Molecular Biomedical Research, Flanders Institute for Biotechnology (VIB), B-9052 Ghent, Belgium
[3]Department of Biomedical Molecular Biology, Ghent University, B-9052 Ghent, Belgium

*Authors for correspondence (jifen.li@jefferson.edu; frans.vanroy@dmbr.vib-UGent.be)
‡These authors contributed equally to this work

Accepted 4 October 2011
Journal of Cell Science 125, 1058–1067

doi: 10.1242/jcs.098640

Summary

It is generally accepted that the intercalated disc (ICD) required for mechano-electrical coupling in the heart consists of three distinct junctional complexes: adherens junctions, desmosomes and gap junctions. However, recent morphological and molecular data indicate a mixing of adherens junctional and desmosomal components, resulting in a 'hybrid adhering junction' or 'area composita'. The α-catenin family member αT-catenin, part of the N-cadherin–catenin adhesion complex in the heart, is the only α-catenin that interacts with the desmosomal protein plakophilin-2 (PKP2). Thus, it has been postulated that αT-catenin might serve as a molecular integrator of the two adhesion complexes in the area composita. To investigate the role of αT-catenin in the heart, gene targeting technology was used to delete the *Ctnna3* gene, encoding αT-catenin, in the mouse. The αT-catenin-null mice are viable and fertile; however, the animals exhibit progressive cardiomyopathy. Adherens junctional and desmosomal proteins were unaffected by loss of αT-catenin, with the exception of the desmosomal protein PKP2. Immunogold labeling at the ICD demonstrated in the αT-catenin-null heart a preferential reduction of PKP2 at the area composita compared with the desmosome. Furthermore, gap junction protein Cx43 was reduced at the ICD, including its colocalization with N-cadherin. Gap junction remodeling in αT-catenin-knockout hearts was associated with an increased incidence of ventricular arrhythmias after acute ischemia. This novel animal model demonstrates for the first time how perturbation in αT-catenin can affect both PKP2 and Cx43 and thereby highlights the importance of understanding the crosstalk between the junctional proteins of the ICD and its implications for arrhythmogenic cardiomyopathy.

Key words: Cardiac intercalated disc, Adherens junction, Desmosome, Plakophilin-2, Gap junction, Connexin43, α-catenin

Introduction

The intercalated disc (ICD) is a highly organized structure located at the termini of cardiomyocytes that maintains structural integrity and synchronizes contraction of cardiac tissue. The ICD is classically defined as containing three distinct junctional complexes: adherens junctions and desmosomes provide strong cell–cell adhesion, and gap junctions electrically couple myocytes. Recently, a novel, exclusive type of 'hybrid adhering junction' or 'area composita' was identified in the mammalian heart (Borrmann et al., 2006; Goossens et al., 2007). Immunoelectron microscopy showed that, in normal mammalian heart muscle, the desmosomal proteins desmoplakin, plakoglobin, plakophilin-2, desmocollin-2 and desmoglein-2, are not restricted to the classic desmosomal junctions as previously thought but are also detected in large adherens-like, but plaque-coated, junctional structures (Borrmann et al., 2006; Franke et al., 2006). Moreover, typical components of the classic adherens junction, including N-cadherin, β-catenin and αE-catenin were shown to colocalize with desmosomal proteins in the majority of the areae compositae (Borrmann et al., 2006; Pieperhoff and Franke, 2007). Interestingly, the area composita is not found in lower vertebrates (Pieperhoff and Franke, 2008), which suggests that it might have evolved to support the increased mechanical load on the mammalian heart by anchoring both actin and intermediate filaments over an extended junctional area at the ICD. The molecular mechanisms that regulate the assembly of this cardiac-restricted mixed-type junctional complex are not known.

N-cadherin is the only classical cadherin expressed in the myocardium, and cardiac-specific knockout of N-cadherin leads to disassembly of the ICD structure and sudden cardiac death (SCD) in mice (Kostetskii et al., 2005; Li et al., 2005). Cadherin-mediated adhesion requires interaction with the actin cytoskeleton by means of various proteins called catenins. Alpha-catenins are key cytoplasmic molecules thought to be indispensable for maintenance of tissue morphogenesis owing to their interaction with, on the one hand, the cadherin-binding partners β-catenin and γ-catenin and, on the other, the actin cytoskeleton (Drees et al., 2005; Yamada et al., 2005). There are three α-catenin subtypes in mammals: αE-catenin, αN-catenin and αT-catenin (Scott and Yap, 2006). All α-catenins contain vinculin-homology domains. αE-catenin is expressed ubiquitously and is essential for early embryonic development (Torres et al., 1997). αN-catenin expression is restricted to neural tissue (Hirano et al., 1992). αT-catenin is a recently identified novel member of the α-catenin family with expression restricted to the

Journal of Cell Science

testis, cardiac muscle and neurons (Janssens et al., 2001; Vanpoucke et al., 2004). αT-catenin and αE-catenin contain vinculin-homology domains and share 57% overall amino acid identity (Janssens et al., 2001; Goossens et al., 2007). Ablation of αE-catenin expression specifically in the mouse heart results in progressive dilated cardiomyopathy (DCM) and susceptibility to cardiac rupture after myocardial infarction (Sheikh et al., 2006). The gene encoding human αT-catenin, *CTNNA3*, has been mapped to chromosome 10q21, a region linked to autosomal dominant familial DCM (Janssens et al., 2003). Although genetic screening has not detected any DCM-linked *CTNNA3* mutations to date, *CTNNA3* is considered a candidate gene and might be the potential cause of this disease (Janssens et al., 2003). More recently, yeast two-hybrid and co-immunoprecipitation showed that αT-catenin interacts directly with desmosomal plakophilin-2 (PKP2) (Goossens et al., 2007), suggesting a unique molecular link between the adherens junctions and desmosomes in the heart. By contrast, αE-catenin lacks plakophilin binding capacity, and the αT-catenin interaction with PKP2 is observed neither for αE-catenin in the heart nor with other plakophilins in epithelial cells (Goossens et al., 2007). The cardiac-tissue-restricted expression and unique interaction with PKP2 support the idea that αT-catenin might mediate the molecular crosstalk between the different junctional complexes of the area composita.

Arrhythmic right ventricular cardiomyopathy (ARVC) is a hereditary heart-muscle disease that causes SCD in young people and athletes (Basso et al., 2009; Saffitz, 2009; Delmar and McKenna, 2010; Sen-Chowdhry et al., 2010). Almost half of the ARVC patients have a mutation in genes encoding cell-adhesion proteins of the desmosome, and hence ARVC is often referred to as a disease of the desmosome. Interestingly, of all five desmosomal genes found to be mutated in ARVC, *PKP2* is the most commonly mutated gene identified in ARVC patients (Gerull et al., 2004; van Tintelen et al., 2006). Importantly, loss of PKP2 expression in cultured cardiomyocytes has been shown to lead to a decrease in total content of the connexin Cx43, redistribution of Cx43 and a decrease in cell–cell communication (Oxford et al., 2007). Gap junction remodeling is associated with SCD in ARVC as well as in other cardiomyopathies. Moreover, the major voltage-gated sodium channel (Nav1.5) is preferentially localized to the ICD, and Nav1.5 function is also regulated by PKP2 (Sato et al., 2009), suggesting multiple mechanisms by which PKP2 might influence electrical conduction in the heart.

In the present study, we utilize a loss-of-function murine model to demonstrate a unique role for αT-catenin in the heart that cannot be compensated for by αE-catenin. Loss of αT-catenin leads to altered PKP2 distribution and to gap junction remodeling. This finding provides a novel paradigm for the crosstalk between the different junctional complexes of the ICD. Finally, we show that αT-catenin-knockout mice are susceptible to ventricular arrhythmias following acute ischemia. We conclude that αT-catenin plays a more important role in the heart than αE-catenin owing to its ability to function as a molecular integrator between adherens junctions and desmosomes at the area composita.

Results

Generation and characterization of αT-catenin-knockout mice

There are two α-catenin subtypes expressed in the myocardium: αE-catenin and αT-catenin (Janssens et al., 2001). Together, they are thought to modulate interactions between the N-cadherin–β-catenin complex and the actin cytoskeleton. Whether these two α-catenins have overlapping and/or distinct functions in the heart is not clear. Hence, we initiated a project to examine the effects of αE-catenin on mechanical coupling of cardiomyocytes in vivo. We generated an inducible cardiac-specific αE-catenin conditional knockout (CKO) by breeding floxed αE-catenin (αE-cat$^{fl/fl}$) mice with inducible αMHC–MERCreMER transgenic mice (Sohal et al., 2001). We observed a marked reduction in αE-catenin expression in the ICD of αE-catenin mutant hearts at 3 months post tamoxifen (Tam) administration (supplementary material Fig. S1A). Cardiac-specific αE-catenin CKO mice exhibited progressive dilated cardiomyopathy approximately 8 months after deletion of the αE-catenin-encoding gene *Ctnna1* (data not shown), consistent with the MLC2v-Cre; αE-cat$^{fl/fl}$ cardiac phenotype reported previously (Sheikh et al., 2006). As αT-catenin can substitute for the adhesive function of αE-catenin in cultured cells (Janssens et al., 2001), we examined αT-catenin expression in the αE-catenin CKO hearts. We observed increased expression of αT-catenin at the ICD in αE-catenin CKO hearts at 3 months post Tam administration (supplementary material Fig. S1B), suggesting that αT-catenin might compensate, at least partially, for loss of αE-catenin in the heart.

The tissue-restricted expression pattern and the ability to interact with desmosomal protein PKP2 suggest that αT-catenin might play a unique role in maintenance of the structural integrity of heart muscle. To investigate the function of αT-catenin in the myocardium, gene targeting technology was used to introduce loxP sites on both sides of exon 3 of *Ctnna3*, encoding αT-catenin (Fig. 1). The αT-catenin floxed mice were mated with Deleter Cre transgenic mice (Schwenk et al., 1995) to generate a germline αT-catenin-null allele. In contrast to αE-catenin-null mice that die in utero (Torres et al., 1997), αT-catenin KO animals are viable, fertile and show no obvious macroscopic phenotypic abnormality. Immunostaining and western blot analysis of αT-catenin KO hearts indicated that the αT-catenin mutation resulted in a null allele (Fig. 2). By comparison, strong αT-catenin staining was found in the ICD of wild-type (WT) heart. A modest increase in αE-catenin (+ 48% vs control; $n=4$; $P<0.05$) was observed in αT-catenin mutant hearts, suggesting possible compensation by αE-catenin in the absence of αT-catenin (Fig. 2). At 3 months of age, the heart-weight:body-weight ratio was moderately increased in αT-catenin KO animals compared with the WT (+18%, $n=8$; $P<0.001$). Histological analysis demonstrated slightly enlarged ventricles in the αT-catenin KO, with no detectable fibrosis at 6 months of age compared with the WT (Fig. 3). Echocardiographic analysis showed an increased left ventricle (LV) internal dimension at the end of systole and diastole, as well as decreased ejection fraction and fraction shortening in the αT-catenin KO at 3 months of age (Fig. 3G). The decrease in cardiac function in the αT-catenin KO mice was not accompanied by a gross morphological change in the ICD structure, as determined by transmission electron microscopy (TEM) of αT-catenin KO hearts at 3 months of age (supplementary material Figs S2, S4). αT-catenin-null mice exhibited earlier onset of dilated cardiomyopathy and cardiac dysfunction compared with either non-inducible (Sheikh et al., 2006) or inducible cardiac-specific αE-catenin CKO (data not shown), which indicates that αT-catenin plays a more important role in maintenance of the organization of the ICD that is crucial for preservation of normal cardiac function.

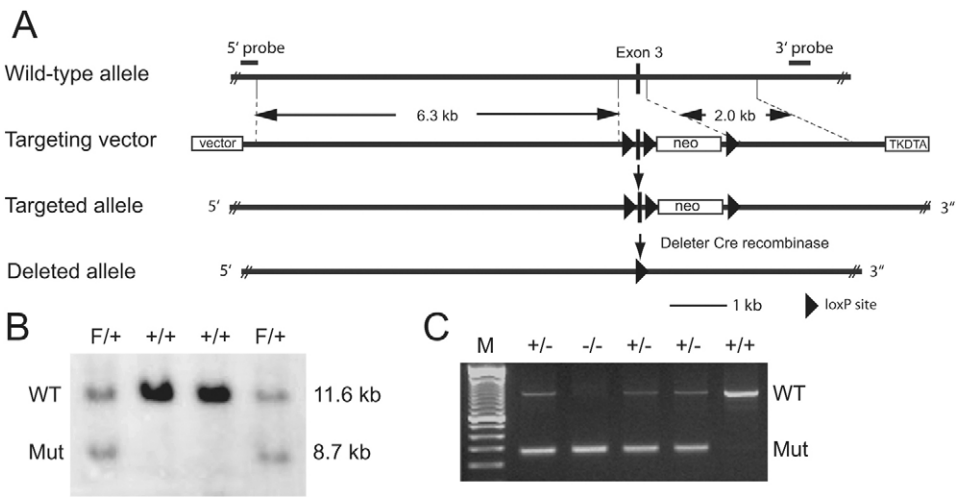

Fig. 1. Generation of a conditional αT-catenin mutation. (**A**) Schematic representation of the expected gene deletion at the αT-catenin locus. LoxP sites are represented by triangles. The targeted allele contains three loxP sites, which flank, respectively, *Ctnna3* exon 3 and the neomycin resistance expression cassette (*neo*). (**B**) A Southern blot analysis of wild-type (WT) (lanes 2, 3) and mutant (Mut) ES cells (lanes 1, 4) is shown. The 3′ probe that was used for screening ES cell clones is indicated in A. (**C**) Mouse tail DNA PCR analysis of the αT-catenin locus of WT (+/+), heterozygous (+/–) and homozygous (–/–) mutant animals after Cre-mediated recombination of the loxP sites.

Reduced PKP2 expression in αT-catenin KO hearts

As part of the N-cadherin–catenin complex, αT-catenin modulates the linkage between the N-cadherin cell-adhesion receptor and the actin cytoskeleton. In addition, recent data indicate that αT-catenin interacts with the desmosomal linker protein PKP2, which suggests that αT-catenin has a unique role in organization of the hybrid adhering junction or area composita (Goossens et al., 2007). To determine the effect of depletion of αT-catenin on the expression of ICD proteins, immunofluorescence analyses were performed on the αT-catenin KO hearts at 6 months of age (supplementary material Fig. S3A,B). Interestingly, the expression levels of adherens junctional (N-cadherin and β-catenin) and desmosomal (plakoglobin and desmoplakin) components were unaltered in the αT-catenin KO hearts. By contrast, desmosomal protein PKP2, which contains a unique binding domain for αT-catenin, showed reduced expression at the ICD of αT-catenin KO hearts (supplementary material Fig. S4). To further evaluate PKP2 cellular expression, cardiomyocytes were isolated from adult αT-catenin KO and WT hearts, and the PKP2-immunoreactive signal at the ICD region was quantified. The amount of specific immunoreactive signal for PKP2 at the ICD region was remarkably decreased in αT-catenin-null compared with WT cardiomyocytes (–67% vs control; $P<0.01$; $n=10$, Fig. 4A). By contrast, no significant change in PKP2 expression was observed at the ICD in αE-catenin CKO hearts (supplementary material Fig. S5).

Cell culture studies using knockdown of PKP2 by small interfering RNA (siRNA) in neonatal rat cardiomyocytes suggest that PKP2 is important for maintaining the area composita (Pieperhoff et al., 2008). To determine whether loss of αT-catenin affects the distribution of PKP2 in the ICD at the ultrastructural level, immunoelectron microscopy was performed for αT-catenin and PKP2 in αT-catenin KO and WT hearts at 5 months of age. The numbers of αT-catenin or PKP2 immunogold-labeled particles at the area composita or desmosome were counted. As shown in Fig. 4B, the area composita was distinguished from the desmosome by possession of less submembranous electron-dense material, absence of the intercellular electron-dense midline structure and positive αT-catenin and PKP2 immunogold labeling. In contrast to WT heart,

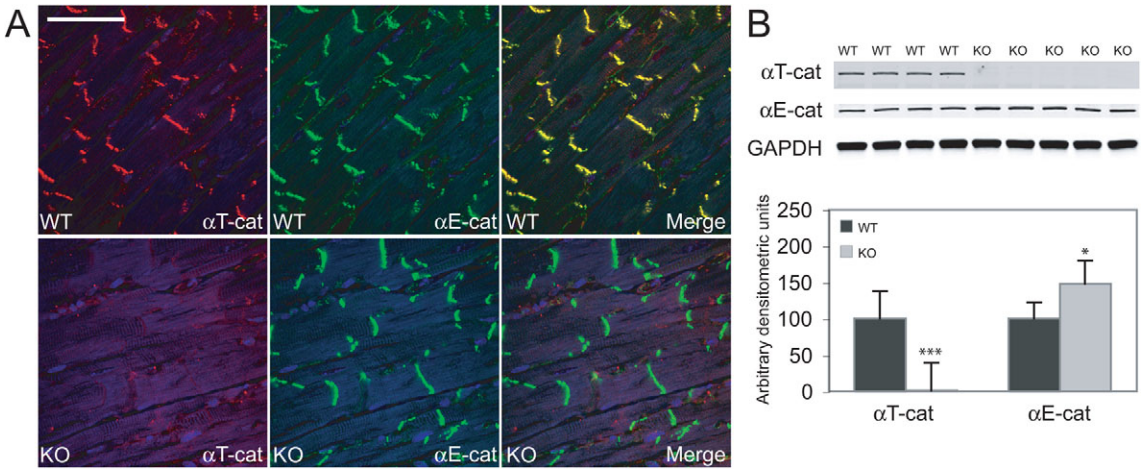

Fig. 2. Expression analysis of αT-catenin and αE-catenin in αT-catenin mutant hearts. (**A**) Hearts from WT and αT-catenin KO animals 3 months of age were immunostained for αT-catenin and αE-catenin. αT-catenin was lost from the intercalated disc (ICD) in the mutant heart. Scale bar: 50 μm. (**B**) Western blot of αT-catenin and αE-catenin in whole-heart lysates from WT and αT-catenin KO mice. αE-catenin expression was significantly increased in αT-catenin mutant hearts. *$P<0.05$; ***$P<0.001$.

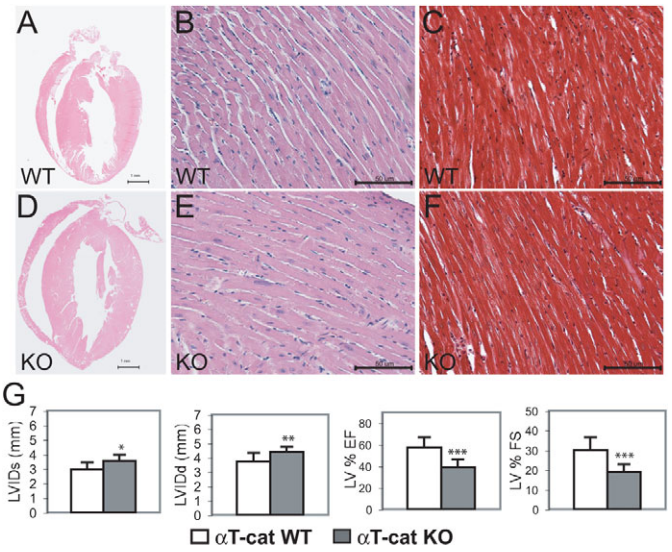

Fig. 3. Histological and cardiac function analysis of αT-catenin mutant hearts. Heart sections from αT-catenin WT (**A**–**C**) and KO (**D**–**F**) animals at 6 months of age. Both ventricles and atria were dilated in the mutant heart (D) compared with the WT (A). Upon staining with Masson's Trichrome (C,F), no apparent fibrosis was seen in the mutant heart. Scale bars: 1 mm (A, D); 50 µm (B, C, E, F). (**G**) Echocardiographic analyses of 3-month-old αT-catenin KO and WT animals. Left ventricular internal dimension at end systole (LVIDs) and diastole (LVIDd) were significantly increased in mutant hearts; LV ejection fraction (LV % EF) and fraction shortening (LV% FS) were significantly reduced in mutant hearts. *P<0.05; **P<0.01; ***P<0.001.

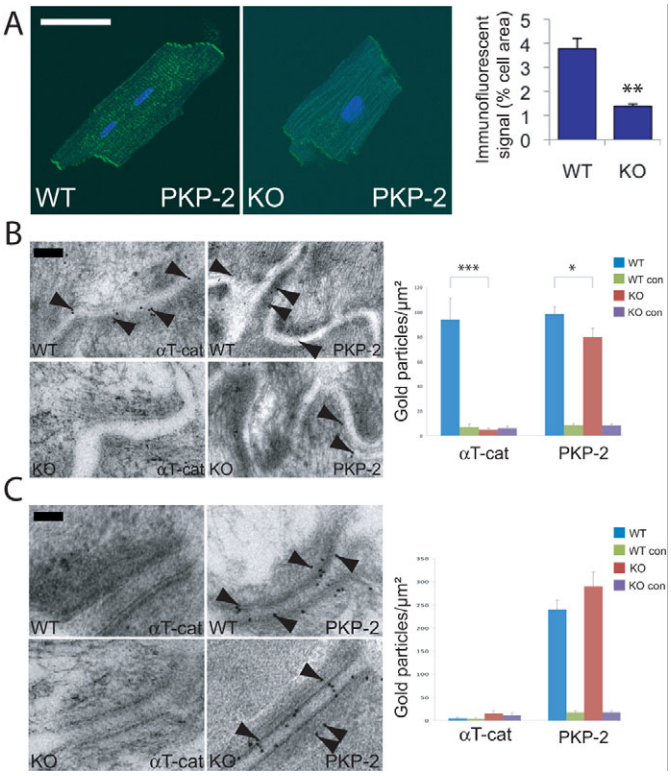

Fig. 4. Reduced PKP2 at the area composita in αT-catenin KO hearts. (**A**) Quantitative confocal analysis for PKP2 expression in adult cardiomyocytes isolated from wild-type (WT) and αT-catenin KO (KO) mice and stained for PKP2. Ten cardiomyocytes from each animal were examined for five or more contiguous pixels of high signal intensity. The amount of specific immunoreactive signal for PKP2 at the ICD was quantified and is shown in the right-hand panel. Scale bar: 50 µm. (**B**,**C**) Immuno-electron microscopy of WT and KO hearts. Representative single immunogold labeling is shown for αT-catenin and PKP2 at either the area composita (B) or at a classical desmosome (C). Right panels: counts of the number of gold particles per µm^2 of junctional area for either areae compositae (B) or desmosomes (C). Note that PKP2 was significantly reduced in areae compositae (B) but not desmosomes (C) of αT-catenin KO heart. Treatment minus primary antibody served as negative controls (WT con and KO con). The error bars in A–C represent the s.e.m. *P<0.05; ** P<0.01; ***P<0.001. Scale bar: 100 nm.

which showed extensive αT-catenin-positive immunogold labeling, αT-catenin was absent from the area composita in the αT-catenin KO heart. Importantly, the number of PKP2-positive immunogold-labeled particles was significantly reduced at the area composita in the αT-catenin KO heart compared with the WT (–19%; P<0.05). However, in desmosomes, recognized in Fig. 4C by their typical electron-dense structure, the number of PKP2-positive immunogold-labeled particles remained unchanged in αT-catenin KO heart compared with the WT. As expected, αT-catenin was not found in desmosomes of either WT or KO heart (Fig. 4C), consistent with our previous report that adherens junctional components are not present in the cardiac desmosome (Goossens et al., 2007).

Gap junction remodeling in αT-catenin KO hearts

We previously demonstrated that decreased N-cadherin levels lead to a reduction in size of large Cx43-containing plaques in the myocardium, accompanied by induced arrhythmia (Li et al., 2008). To examine whether loss of αT-catenin affects Cx43-containing gap junction plaques, western blot analysis and immunofluorescence microscopy were performed in situ (supplementary material Fig. S6B,C) and on cardiomyocytes isolated from adult αT-catenin KO mice (Fig. 5). To determine the number and size of gap junction plaques, we used a minimal junction size of five or more contiguous pixels and compared the signal intensity between αT-catenin KO and WT cardiomyocytes. The immunofluorescent signal for Cx43 was significantly reduced (–76% vs control; P<0.01; n=10) in αT-catenin-deficient cardiomyocytes compared with the WT (Fig. 5A). Importantly, both the number and size of Cx43-containing gap junctions were significantly decreased in the αT-catenin KO cardiomyocytes compared with the WT (–36% vs control, P<0.05 for number; –67% vs control, P<0.01 for size; n=10) (Fig. 5A). By contrast, no significant change in Cx43 expression was observed in αE-catenin CKO hearts (supplementary material Fig. S6A), consistent with a previous report (Sheikh et al., 2006). Furthermore, immunoelectron microscopy revealed a significant reduction in gap junction length, determined by Cx43 immunogold labeling (Fig. 5B) (1.698±0.19, n=20 for WT, 0.938±0.12, n=15 for KO, P<0.01). To elucidate further the cellular distribution of Cx43 in the ICD region, the colocalization between Cx43 and N-cadherin was examined in isolated adult cardiomyocytes by quantitative confocal microscopy (Fig. 6). N-cadherin was not significantly changed in αT-catenin-deficient cardiomyocytes (supplementary material Fig. S3A); therefore, N-cadherin could serve as a marker of the ICD. In WT cardiomyocytes, strong positive correlations for colocalization between Cx43 and N-cadherin were indicated by Pearson correlation coefficient (rp) values of 0.45 and Spearman

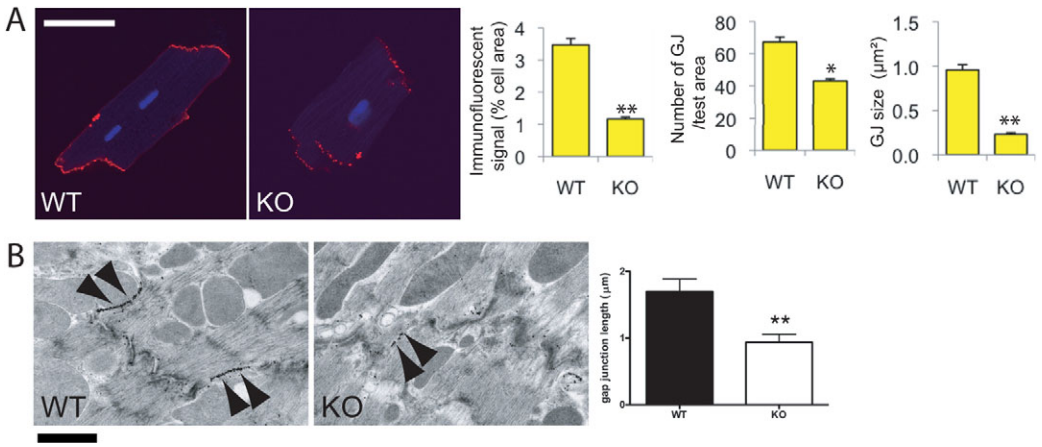

Fig. 5. Reduced Cx43 expression at the ICD of αT-catenin KO hearts. (**A**) Adult cardiomyocytes isolated from WT and αT-catenin KO hearts were immunostained for Cx43. Ten cardiomyocytes from each animal were examined for five or more contiguous pixels of high signal intensity. The amount of specific immunoreactive signal at ICDs for Cx43, the number of Cx43-containing plaques (gap junction, GJ) and their size (GJ size) were quantified and are shown in the panels at the right. Scale bar: 50 μm. (**B**) Single immunogold labeling of Cx43 with silver amplification at representative gap junctions of the ICD from WT and αT-catenin KO hearts. Arrowheads point to typical immunopositive signals. Right panel: the length of gap junctions was measured in the hearts. The error bars represent the s.e.m. *, $P<0.05$; **, $P<0.01$. The number of gold particles per μm of gap junction did not differ significantly between the WT and the KO heart (data not shown). Scale bar: 1 μm.

correlation coefficient (*r*s) values of 0.49 (Fig. 6A). By contrast, in the absence of αT-catenin, the colocalization of Cx43 and N-cadherin at the ICD was significantly reduced, as indicated by *r*p values of 0.20 and *r*s values of 0.25 (Fig. 6B). Moreover, adult cardiomyocytes were co-stained with antibodies against Cx43 and PKP2, and colocalization was quantified. Pearson and Spearman colocalization coefficient and scatter plot (sp) analysis also revealed reduced colocalization between Cx43 and PKP2 in αT-catenin KO cardiomyocytes (*r*p =0.38, sp=0.40 in WT; *r*p=0.17, sp=0.14 in KO). Collectively, these data demonstrate that αT-catenin is required to maintain large gap junction plaques at the ICD, which might be mediated through an αT-catenin–PKP2–Cx43 multiprotein complex.

αT-catenin KO mice exhibit increased susceptibility to ischemia-induced arrhythmias

Gap junction remodeling often leads to abnormal electrical conduction properties and subsequent arrhythmias. Therefore, αT-catenin KO hearts were examined for electrical irregularities under normal and stressed conditions. Electrophysiological analysis based on volumetric ECG recordings did not detect a significant change in the PR intervals (42.3 milliseconds ± 3.3, $n=14$ for KO vs 42.4 milliseconds ± 2.9, $n=6$ for WT) or QRS complex widths (13.0 milliseconds ± 1.0, $n=14$ for KO vs 16.4 milliseconds ± 1.4, $n=6$ for WT). This result indicates the apparent absence of a conduction abnormality in the αT-catenin KO mice under normal conditions. To determine whether the

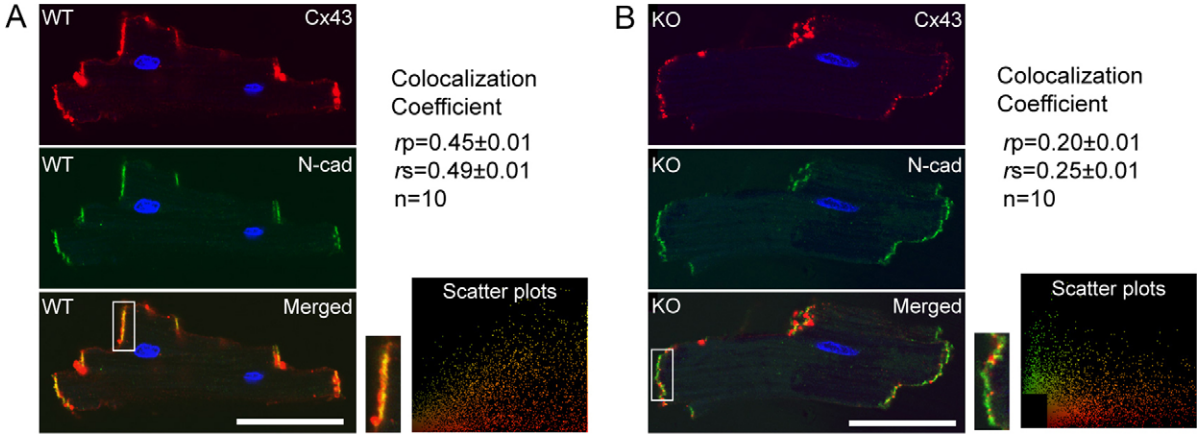

Fig. 6. Reduced colocalization of Cx43 with N-cadherin in the ICD of αT-catenin KO heart. Adult cardiomyocytes ($n=10$) isolated from either WT or αT-catenin KO mice were co-stained for Cx43 (red) and N-cadherin (green). Boxed regions in the merged images are also shown at higher magnification. The images were analyzed by using ImageJ software with a Pearson–Spearman correlation colocalization plug-in to perform quantitative statistical colocalization on the two-color confocal images, as described previously (French et al., 2008). (**A**) In images of WT cells, strong positive correlations for colocalization between Cx43 and N-cadherin in the ICD were indicated by an *r*p value of 0.45 and an *r*s value of 0.49. (**B**) In images of αT-catenin KO cells, reduced colocalization between Cx43 and N-cadherin in the ICD was indicated by an *r*p value of 0.20 and an *r*s value of 0.25. Scale bars: 50 μm.

animals were susceptible to induced arrhythmias, ventricular programmed electrical stimulation was performed on the hearts. Burst ventricular pacing at a cycle length of 50 milliseconds did not induce arrhythmias in the αT-catenin KO (none of 14) or WT (none of six) hearts. By contrast, the induction of arrhythmias in N-cad$^{-/+}$; Cx43$^{-/+}$ hearts (three of four), as reported previously (Li et al., 2008), confirms the effectiveness of the stimulation protocol. Owing to differences in cardiac electrophysiology between mouse and larger mammals, it is often difficult to induce arrhythmias in mice without further stress, such as cardiac injury. So, it has been shown that, after acute ischemia, diminished electrical coupling caused by reduced expression of Cx43 accelerates the onset and increases the incidence of ventricular arrhythmias (Lerner et al., 2000). To determine whether depletion of αT-catenin enhances arrhythmogenesis in ischemia-reperfusion (I-R) injury, left anterior descending (LAD) coronary artery ligation was performed to induce I-R injury in αT-catenin KO and WT mice. To avoid any secondary effects due to cardiac remodeling in the mutant hearts, surgery was performed on 2.5-month-old αT-catenin KO animals prior to the onset of cardiomyopathy. To monitor ECG after I-R, miniature telemetry transmitter devices were implanted in the animals before I-R. Heart rhythms were monitored especially during the 30-minute ischemia and 24 hours post I-R. Premature ventricular contractions (PVCs) are ectopic contractions that originate from the ventricles. PVCs are the most commonly seen ventricular arrhythmia due to insufficient coronary blood supply during acute ischemia (Gao et al., 2010). Representative telemetry ECGs (Fig. 7A) illustrate different patterns of PVCs following I-R. In comparison with WT animals, αT-catenin KO mice exhibited a significant increase in the number of PVCs (KO 75.7±6.6; WT 4.2±2.0; sham-operated 0.7±0.3; $P<0.001$ between groups) and short ventricular tachycardia (VT) (KO 4.6±1.4; WT 0.2±0.2; sham-operated 0±0; $P<0.05$ between groups) after I-R (Fig. 7B). Next, ECG parameters were analyzed especially during the first 12-hour overnight period post I-R. The durations of QRS, QTc, RR and ST intervals were averaged from at least 100 beats recorded in sham-operated, WT and KO animals. Although QRS and ST intervals tended to be longer in the KO I-R group, the values did not reach statistical significance (Fig. 7C). Notably, the QTc interval was prolonged by ~16% in αT-catenin KO animals compared with the WT (KO 62.5±4.1; WT 54.4±4.1; sham-operated 53.8±1.1; $P<0.01$ KO vs WT, $P<0.001$ KO vs sham-operated) post I-R. Although only two out of 39 mice were found dead at days 3 and 4 following I-R, both of them were αT-catenin KO mice (KO $n=21$; WT $n=18$). These findings indicate that, even before the development of cardiac pathology, there is an increased risk of significant and potentially fatal ventricular arrhythmias in αT-catenin KO mice following I-R.

Discussion

Dilated cardiomyopathy (DCM) is the most common form of myocardial disease, and it is associated with a high incidence of ventricular arrhythmia, severe congestive heart failure and an increased risk of sudden death. Although the human αT-catenin gene *CTNNA3* has been mapped to chromosome 10q21, a locus linked to autosomal dominant familial DCM (Janssens et al., 2003), its function in the working myocardium has not been determined. In the present study, we demonstrate for the first time the unique role of αT-catenin as the molecular linker required for the maintenance of the hybrid adhering junction or area composita in the heart. Disruption of the area composita in the αT-catenin KO mice leads to early onset of DCM, gap junction remodeling and an increased susceptibility to ventricular arrhythmia in the setting of I-R injury.

With the recent identification of the area composita (Borrmann et al., 2006; Franke et al., 2006), there is considerable interest in understanding the molecular organization of this unique junctional complex found exclusively in the cardiac ICD. Among the various adhesion junction components, PKP2 has been implicated in the formation, architectural organization and stability of these hybrid junctions. Indeed, germline deletion of

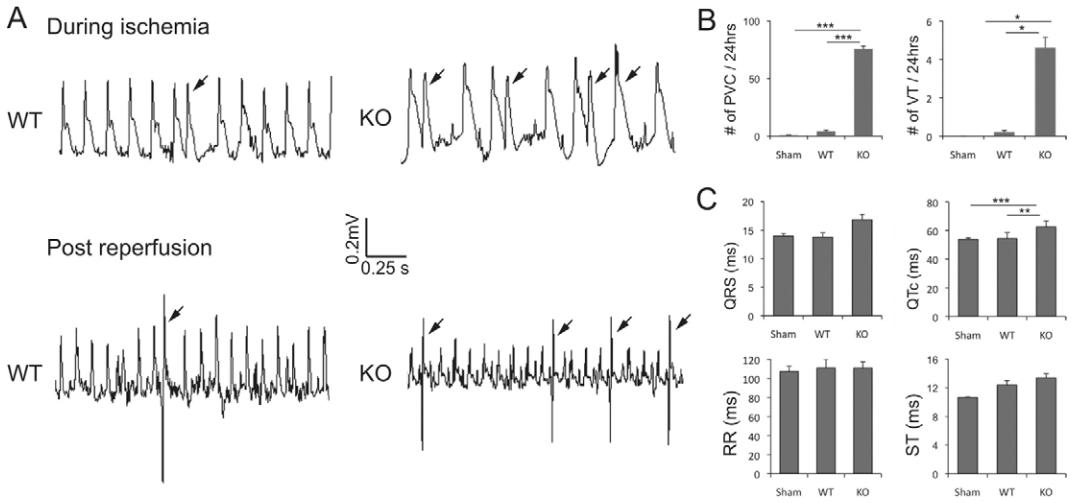

Fig. 7. Telemetry ECG recordings in αT-catenin KO mice post ischemia-reperfusion (I-R) injury. Mice from WT and αT-catenin KO, 2.5 months of age, were subjected to ligation of the left anterior descending coronary artery for 30 minutes and 7 days reperfusion. A miniaturized telemetry ECG transmitter was implanted before I-R. (**A**) Representative telemetry ECGs of different patterns of premature ventricular contractions (PVCs; arrow) during I-R injury in WT and αT-catenin KO mice. (**B**) PVCs and ventricular tachycardia (VT) counted from ECG recordings acquired for 5 minutes every 15 minutes for 24 hours after ischemia (sham-operated $n=7$, WT $n=5$, KO $n=10$). (**C**) ECG parameters analyzed during the 12-hour overnight period post I-R (sham-operated $n=7$, WT $n=4$, KO $n=7$). The error bars represent the s.e.m. *$P<0.05$; **$P<0.01$; ***$P<0.001$.

PKP2 in mice results in mid-gestation lethality due to disruption of the myocardial cytoarchitecture (Grossmann et al., 2004). Furthermore, knockdown of PKP2 in neonatal cardiomyocytes resulted in remodeling of the area composita structure (Pieperhoff et al., 2008). Hence, it was remarkable that the expression and distribution of adherens junction and desmosome proteins were not affected in the αT-catenin KO heart, with the exception of PKP2. This result is consistent with data from yeast two-hybrid and co-immunoprecipitation experiments that demonstrated that αT-catenin interacts directly with PKP2 through its adhesion modulation domain (amino acids 496–576) (Goossens et al., 2007). In contrast to αT-catenin, αE-catenin and αN-catenin do not contain a functional PKP2 binding domain. Hence, as might be predicted, we did not observe a change in PKP2 expression or distribution in αE-catenin CKO hearts. Importantly, immuno-EM showed that PKP2 was decreased at the area composita in the αT-catenin KO hearts, whereas its normal expression was retained at the desmosome. The retention of PKP2 at the desmosome in the absence of αT-catenin is consistent with the association of PKP2 with desmosomal cadherins in both desmosomes and areae compositae, whereas αT-catenin associates only with the N-cadherin–catenin complex located in the area composita. As determined by TEM, the overall ICD structure appeared remarkably normal in the αT-catenin KO mice at 3 months of age, indicating that the loss of αT-catenin and the decreased level of PKP2 in the area composita were not sufficient to elicit a significant structural change in the ICD. The combination of adherens junctional and desmosomal components allows actin and desmin, respectively, to be anchored at the area composita to create a reinforced adhesive junction. This novel hybrid junction configuration is thought to provide additional mechanical strength to the mammalian cardiac ICD structure. If this were true, a simple prediction is that, compared with knockout of αE-catenin, depletion of αT-catenin would affect to a greater extent the structural integrity of the heart. Indeed, this is the case, as the αT-catenin KO mice developed cardiomyopathy significantly earlier than αE-catenin CKO mice (3 vs 8 months of age) (Sheikh et al., 2006). Collectively, these data support the notion of there being a specific molecular interaction between the adherens junction protein αT-catenin and the desmosomal protein PKP2 and thus demonstrate that αT-catenin, not αE-catenin, is the crucial integrator molecule between the different junctional complexes in the area composita.

Interestingly, PKP2 has been reported to interact, most probably indirectly, with Cx43 in both testis (Li et al., 2009) and heart (Oxford et al., 2007) – two tissues that express high levels of αT-catenin (Janssens et al., 2001). Co-immunoprecipitation and GST pulldown assay showed that PKP2 associated with Cx43 to form a macromolecular complex in rat heart lysate (Oxford et al., 2007). Importantly, knockdown of PKP2 expression in cultured cardiomyocytes results in remodeling of gap junction plaques that contain Cx43 (Oxford et al., 2007). Our current study demonstrates that loss of αT-catenin leads to a significant decrease in the amount of immunoreactive signal of both PKP2 and Cx43 in the ICD, as well as a reduction in colocalization of N-cadherin and Cx43 in the ICD. In contrast, no significant difference in PKP2 or Cx43 levels was observed in the αE-catenin CKO heart [supplementary material Figs S5, S6 (Sheikh et al., 2006)]. These data suggest that αT-catenin might act synergistically with desmosomal PKP2 to stabilize gap junctions at the ICD.

Accumulating evidence indicates the importance of mechanical junctions in the regulation of gap junction assembly and organization (Saffitz, 2006). However, the exact mechanism(s) by which adhesion proteins influence connexon trafficking, channel assembly and/or stability at the ICD is poorly understood. Of potential relevance to our study, it was recently demonstrated that PKP-2 regulates the cytoskeletal scaffold protein ankyrin-G (AnkG) in cultured cardiomyocytes (Sato et al., 2011). Importantly, the authors showed that knockdown of AnkG led to a decrease in Cx43 and a reduction in the extent of electrical coupling between cardiomyocytes (Sato et al., 2011). Thus we can speculate that disruption of the area composita in the αT-catenin KO hearts weakens the actin and the desmin cytoskeletal networks, resulting in a reorganization of the cytoskeleton, including scaffold proteins such as AnkG, and leading to gap junction remodeling. Future experiments will be necessary to address this and other alternative possibilities.

It is well established from human diseased myocardium and animal models that altered gap junction expression referred to as gap junction remodeling contributes to the arrhythmogenic substrate. The importance of Cx43 regulation of arrhythmia susceptibility in the acute ischemic heart has been shown in both heterozygous Cx43 KO mice (Lerner et al., 2000) and mice with a carboxyl-terminal domain truncation of Cx43 (Maass et al., 2007). A reduced amount and organization of Cx43-containing gap junction plaques probably plays a fundamental role in the increased incidence of arrhythmias observed in these two mouse models. Based on those studies, we speculate that the diminished levels of gap junctional Cx43 in the ICD of αT-catenin-ablated cardiomyocytes, as well as the reduced number and size of Cx43-containing gap junction plaques in αT-catenin KO cardiomyocytes in vitro and in vivo, might lead to an increased incidence of arrhythmias. Indeed, αT-catenin KO mice exhibited a higher frequency of occurrence of ventricular premature contraction and ventricular tachycardia following acute ischemia.

Mechanisms that mediate uncoupling in ischemia are related to multiple pathophysiological processes, including increased levels of intracellular ions (Dekker et al., 1996), intracellular acidosis (Yan and Kleber, 1992) and accumulation of lipid metabolites (Massey et al., 1992). Importantly, although reperfusion is essential to prevent irreversible cellular injury and preserve ventricular function, reperfusion and the attendant recovery from ischemia can cause ventricular arrhythmias, cellular injury and SCD (Pogwizd and Corr, 1987). In this regard, it is important to emphasize the increased susceptibility to ventricular arrhythmia observed during the first 24 hours of reperfusion in αT-catenin KO animals in comparison with WT animals. Long QT syndrome has been associated with a frequent occurrence of PVCs and SCD (Chopra and Knollmann, 2011). During the first 12 hours of overnight ECG analysis, significantly increased QTc was observed in αT-catenin KO animals post I-R. Therefore, dysregulation of ion channels might be involved in the increased arrhythmogenesis in the ischemic αT-catenin KO heart. Recent evidence indicates that alteration of mechanical junctions can affect ion-channel function. Of particular relevance to our studies, knockdown of PKP2 in cultured cardiomyocytes caused slowing of conduction, coincident with altered functioning of the Nav1.5 channel (Sato et al., 2009). Moreover, aberrant Kv1.5 channel function might contribute to the arrhythmogenic phenotype in N-cadherin CKO mice (Cheng et al., 2011), further supporting the functional interplay between

the different mechanical junctions and ion channels located at the ICD. In the future, it will be of interest to examine ion-channel function in the αT-catenin KO cardiomyocytes.

The area composita is a unique hybrid-type adhesive junction found exclusively in the heart of higher vertebrate species (Pieperhoff and Franke, 2008). It is probably more than a coincidence that fish (*Danio rerio*) and amphibians (*Xenopus laevis*) lack the area composita in the heart and do not contain the gene encoding αT-catenin, whereas both species contain genes encoding αE-catenin and αN-catenin (Zhao et al., 2011). Evolutionary comparison of the three α-catenin genes indicates that the αT-catenin gene arose from an amniote-specific duplication of the common ancestor, the gene encoding αN-catenin (Zhao et al., 2011) (and J.L., S.G. and J.v.H. et al., unpublished). In addition to its presence in mouse (*Mus musculus*), the αT-catenin gene can be found in the lizard *Anolis carolinensis*, the chicken *Gallus gallus* and human genomes. Although less common than in mouse, mixing of adherens junction and desmosome components has been observed in chick heart muscle (Pieperhoff and Franke, 2008). It is possible that upon gene duplication, a gene encoding αT-catenin evolved as it was of selective advantage for formation of a hybrid adhering junction or area composita in the heart of amniotes. In addition, it is important to note that αT-catenin is found in amniotes that have a four-chambered heart, whereas it is absent in amphibians that have a three-chambered heart. It is interesting to speculate that the septation of the ventricle in terrestrial vertebrates required a novel more extended hybrid-type junction to support the mechanical load needed to pump blood effectively throughout the pulmonary and systemic circulations. A detailed analysis of the expression pattern of αT-catenin during chamber development in amniotes, particularly the right ventricle, might prove informative for our comprehension of the evolution of the four-chambered heart.

Mutations in the genes encoding five desmosomal proteins of the ICD are responsible for almost half of the mutations linked to the cardiomyopathy ARVC, an inherited disease associated with ventricular arrhythmias and SCD in the young (Basso et al., 2009; Saffitz, 2009; Delmar and McKenna, 2010; Sen-Chowdhry et al., 2010). Alterations in the molecular interactions between the junctional complexes in the area composita might play an important role in the pathogenesis of ARVC. Given the large number of *PKP2* mutations identified in ARVC patients (Gerull et al., 2004; van Tintelen et al., 2006), it will be of interest to determine whether any of the ARVC-causing mutations disrupt the interaction between PKP2 and αT-catenin. A better understanding of the molecular interactions at the area composita might help explain the variable expressivity of cardiac phenotypes observed in ARVC patients with desmosomal gene mutations, especially those carrying *PKP2* mutations. ARVC patients were recently identified with more than one mutation in the same or different desmosomal gene, suggesting that ARVC might require multiple genetic hits in the cell-adhesion complex to elicit a cardiac phenotype (den Haan et al., 2009; Bauce et al., 2010; Xu et al., 2010). Our genetic studies indicate that αT-catenin is a potential genetic modifier of the ARVC phenotype. Future genetic analyses will be necessary to address this possibility.

In conclusion, our study provides in vivo evidence for a unique role for αT-catenin as a molecular integrator of adherens junctional and desmosomal components at the area composita. Disruption of this link in αT-catenin KO mice results in early onset of DCM, gap junction remodeling and increased risk of cardiac arrhythmia. In the future, it will be of interest to determine whether αT-catenin is affected in ARVC patients, and, if so, whether changes in αT-catenin influence the incomplete penetrance and variable expressivity of this disease.

Materials and Methods

Generation of T-catenin targeting vector

Clone 184N16 was identified by PCR screening of a mouse genomic BAC library (Genome Systems, St Louis, MO) using primers MCBU#2838 (5′-CCGC-AGAATCCTTCCAACA-3′) and MCBU#2839 (5′-GCTGCCAGCTCTTCC-TTTAAA-3′). Of this BAC clone, a 9.0-kbp *Sac*I fragment containing *Ctnna3* exon 3 was subcloned into the pGEM11 vector (Promega) and sequenced. This subclone was used as backbone to construct a conditional mouse *Ctnna3* targeting vector through two consecutive Red–ET-cloning steps (Gene Bridges, Heidelberg, Germany) in DY380 bacteria with temperature-inducible Redγ expression. In a first ET-cloning step, a PCR-amplified floxed kanamycin–neomycin resistance cassette was inserted by recombination in mouse *Ctnna3* intron 2. The resultant plasmid was electroporated into bacteria expressing Cre recombinase (strain 294-Cre) (Buchholz et al., 1996). This removed the selection cassette but left one residual loxP site upstream of exon 3. This construct was then used for a second ET-cloning. This time, the PCR-amplified floxed kanamycin–neomycin resistance cassette was inserted in intron 3 to generate plasmid pGEM11-maT-catenin-cKO, containing three loxP sites flanking the mouse *Ctnna3* exon 3 and the neomycin resistance cassette (Fig. 1A). For amplification of the kanamycin–neomycin cassette of the first ET cloning, primers with the following sequences were used: MCBU#3748 (5′-CCACTGAGCCACACCAGCTGTGTACTGCCCACCTCCA-TTTTTCCCTTCCT-GATATC-TCTGCAAACCCTATGCTACTCCGTC-3′) and MCBU#3749 (5′-TAGATGAAGGCCTGAGAGGACCATGGTGCATCATATA-CTTACTGTGGAAAATCCCGGCGGATTTGTCCTACTCAGGAGAGCG-3′). For amplification of the kanamycin–neomycin cassette of the second ET cloning, the following primers were used: MCBU#3805 (5′-CCCCTAA-TAACCGAAGAGAGGCTGATGGTGTGGACGATGCCTTCACCCATA-GATATC-TCTGCAAACCCTATGCTACTCCGTC-3′) and MCBU#3806 (5′-CTA-TTTTTGAGGCTGTCGGGGAGGAAGTGTTTAACTGCTTACAGAGAACTT-TCCCGGCGGATTTGTCCTACTCAGGAGAGCG-3′). Primers MCBU#3748 and MCBU#3805 contain extra *Eco*RV restriction recognition sites, which were used to screen for positive recombination in *Escherichia coli* and later in mouse ES cells. Finally, to minimize random integration, a negative selection cassette (PGK-diphtheria toxin A; DTA) was inserted by conventional cloning into the *Xho*I site downstream of the short homology domain in intron 3.

ES cell targeting, Southern blot screening and generation of chimeras

ES cells (129S6/SvEvTac) were grown and manipulated as described previously (Schoonjans et al., 2003). The αT-catenin targeting vector was linearized with *Not*I and electroporated in ESMO ES cells. A total of 350 neomycin-resistant ES clones were screened by Southern blotting for correct recombination. Correct 5′ recombination was tested with a 5′ external probe (15.8 kbp WT allele fragment and 13.6 kbp targeted allele fragment) and a neomycin-resistance gene probe (3.3 kbp targeted allele) on *Eco*RV-digested genomic DNA (gDNA). Correct 3′ integration was confirmed using a 3′ external probe (11.6 kbp WT allele fragment and 8.7 kbp targeted allele fragment) on *Bgl*I-digested gDNA. The 5′ probe was amplified by PCR on genomic ES cell DNA using primers MCBU#3581 (5′-CCCAGAGTACCATTTTCAAC-3′) and MCBU#3582 (5′-GTCGGAGCTTG-TGATTTAAT-3′) and cloned in pGEMTe according to the manufacturer's guidelines. The 3′ probe was amplified using primers MCBU#3752 (5′-CGA-GGAATGCTTTCTGTATG-3′) and MCBU#3753 (5′-CAGGGAAAACATGC-AGTCTA-3′). For the internal neomycin-resistance gene probe, a *Bgl*II-*Nco*I fragment of pPGK-Neo-loxP (Gene Bridges) was used. Correctly targeted ES cells were injected into blastocysts and transferred to pseudopregnant females.

Immunofluorescent staining of heart tissue

Hearts were isolated and fixed in 4% formaldehyde freshly prepared from paraformaldehyde, dehydrated and embedded in paraffin. Sections (6 μm) were cut, mounted, dewaxed in xylene, rehydrated through an ethanol series and then heated in 1× Antigen Unmasking Solution (Vector Laboratories, Burlingame, CA) in a microwave oven (350 W) for 10 minutes to unmask the epitope. After blocking with 5% nonfat milk in PBS for 30 minutes, sections were incubated at 4℃ for 16 hours with primary antibodies diluted in 5% nonfat milk in PBS. The primary antibodies used were against the following proteins: N-cadherin (3B9, Invitrogen, Carlsbad, CA), β-catenin (CAT-5H10, Invitrogen), αE-catenin (C2081, Sigma, St Louis, MO), αT-catenin (Janssens et al., 2001), plakoglobin (clone 15, BD Biosciences, San Jose, CA), desmoplakin (multi-epitope cocktail, ARP, Waltham, MA), plakophilin-2 (clone 2a+2b, Fitzgerald, Acton, MA), Cx43 (clone C6219, Sigma). After washing in PBS, sections were incubated with Alexa-Fluor-488- or 555-conjugated goat anti-mouse or rabbit antibody (Invitrogen) for 1 hour

at room temperature. The sections were washed in PBS and mounted using Prolong Gold Antifade reagent containing DAPI. Slides were dried overnight and imaged with a Zeiss LSM 510 META Confocal Microscope System (Carl Zeiss, Maple Grove, MN) at room temperature (23℃) with a Plan Apochromat ×63 1.4-NA oil objective. Linear adjustments of brightness and contrast levels were applied in ImageJ. Figures were assembled in Adobe illustrator CS.

Western blotting

Hearts were homogenized in a modified RIPA buffer (50 mM Tris-HCl pH 7.5, 150 mM NaCl, 1 mM EDTA pH 8.0, 1% NP-40, 0.5% Na deoxycholate, 0.1% SDS) containing proteases inhibitors and phosphatase inhibitor cocktails I and II (Roche Diagnostics, Indianapolis, IN) and centrifuged at 12,000 ***g*** for 15 minutes. Western blot analyses were performed with the antibodies described above. For normalization of signals, blots were also analyzed with anti-GAPDH monoclonal antibodies (clone 6C5, RDI, Acton, MA), followed by IRDye-680- or IRDye-800CW-conjugated secondary antibody (LI-COR, Lincoln, NE). Membranes were imaged with Odyssey Infrared Imaging System (LI-COR), and quantitative densitometric analysis was performed with Odyssey version 1.2 infrared imaging software.

Histological analysis

Hearts were isolated and fixed in 4% formaldehyde freshly prepared from paraformaldehyde, dehydrated and embedded in paraffin. Global heart architecture was determined from longitudinal 6-µm deparaffinized sections stained with hematoxylin and eosin (H&E). Fibrosis was detected with Masson's Trichrome staining. All imaging was performed at room temperature (23℃) with a Nikon Eclipse 80i and a Plan Apochromat ×20 0.75-NA dry objective. NIS-Elements software was used for image analysis. Figures were assembled in Adobe illustrator CS.

M-mode, two-dimensional echocardiography

Transthoracic two-dimensional echocardiography (TTE) was performed with a Vevo 770 high-resolution imaging system equipped with a 30-MHz probe (Visual Sonics, Toronto, Canada) on anesthetized (2% inhaled isoflurane) WT and KO mice. LV wall thickness and dimensions were measured from M-mode images at the plane bisecting the papillary muscles. Values were obtained by averaging three consecutive cardiac cycles, and ventricular fractional shortening and ejection fractions were calculated.

Electron microscopy analyses

For morphological analysis, mouse heart tissue was excised, briefly immersed in 20% (w/v) BSA and frozen immediately in a high-pressure freezer (EM Pact, Leica Microsystems, Vienna, Austria). Freeze-substitution in dry acetone containing 0.1% uranyl acetate, 1% (w/v) OsO_4 and 0.2% glutaraldehyde was performed in a Leica EM AFS for four days as follows: –90℃ for 26 hours, 2℃ per hour increase for 15 hours, –60℃ for 8 hours, 2℃ per hour increase for 15 hours and –30℃ for 8 hours. Samples were then slowly warmed up to 4℃, infiltrated stepwise over 3 days at 4℃ in Spurr's resin and embedded in capsules. Polymerization was performed at 70℃ for 16 hours. Ultrathin sections were cut with an ultramicrotome (Leica EM UC6) and post-stained in a Leica EM AC20 for 40 minutes in uranyl acetate at 20℃ and for 10 minutes in lead stain at 20℃. Grids were viewed with a JEM 1010 transmission electron microscope (JEOL, Tokyo, Japan) operating at 80 kV. For immuno-EM, mouse heart tissue was excised, briefly immersed in Ringer's solution with 3% sucrose and frozen immediately in a high-pressure freezer (HPM010, Bal-Tec AG, Liechtenstein). Freeze-substitution was carried out in a Leica EM AFS 1. Heart tissue was substituted in dry acetone with 0.5% uranyl acetate as follows: –85℃ for 18 hours, 7℃ per hour increase for 5 hours up to –50℃, washing in pure ethanol for 1 hour, 33% Lowicryl HM-20 in ethanol for 1 hour, 66% Lowicryl HM-20 in ethanol for 1 hour and two times 4 hours in 100% Lowicryl HM-20. Polymerization was performed by UV illumination for 24 hours at –50℃ followed by 24 hours at −35℃. Immunolabeling and label quantification were performed as described previously (Goossens et al., 2007). The following primary antibodies were used for immuno-EM: rat monoclonal mouse αT-catenin-specific antibody 1159_12A4S4 (diluted 1:10) (Janssens et al., 2001), mouse monoclonal PKP2-specific antibody (1:10; Progen, Heidelberg, Germany) and Cx43-specific antibody (1:50; Sigma).

Isolation of adult cardiomyocytes and quantitative immunocytochemistry analysis

Mouse ventricular myocytes were isolated from adult WT and KO mice (5–6 months old) after dissociation with collagenase B, collagenase D and protease, as described previously (Li et al., 2008). Cells were then fixed in 4% formaldehyde freshly prepared from paraformaldehyde for 20 minutes and subsequently suspended in PBS for immunostaining as described previously (Li et al., 2008). The primary antibodies used are described above. The images were captured on a Zeiss LSM 510 META Confocal Imaging System as described above and the amount of immunoreactive signal at the ICD was analyzed with NIH ImageJ as described previously (Li et al., 2008). In addition, using a Pearson–Spearman correlation colocalization plug-in, quantitative statistical colocalization on the two-color confocal images was performed between N-cadherin or PKP2 and Cx43, as described by French and colleagues (French et al., 2008).

Electrophysiology studies in isolated hearts

Adult mice were heparinized (0.5 U g^{-1} IP) and then anesthetized with Avertin (100 mg kg^{-1} IP). The hearts were quickly removed through a thoracotomy and rinsed in a Tyrode's solution containing (in mmoles l^{-1}) NaCl 130, $NaHCO_3$ 24, NaH_2PO_4 1.2, $MgCl_2$ 1.0, glucose 5.6, KCl 4.0 and $CaCl_2$ 1.8, equilibrated with a 95% O_2, 5% CO_2 gas mixture. Hearts were then rapidly cannulated, perfused in a retrograde fashion by means of an aortic cannula with 37℃ oxygenated Tyrode's solution (2–3 ml $minute^{-1}$) and placed in a chamber. The solution in the chamber was used as a volume conductor for recording ECGs. ECGs were recorded with a Cyber Amp380 amplifier (Axon Instruments) and digitized at 10 kHz with a Digidata 1400A and Axoscope 10.2 after equilibration for 20 minutes. Bipolar pacing electrodes were placed on the epicardium of the ventricle. The ventricle was paced with pulses equivalent to 1.5× threshold amplitude with a 2 millisecond duration.

Surgical induction of myocardial ischemia-reperfusion injury

All animal procedures and experiments were performed in accordance with the guidelines of the Institutional Animal Care and Use Committee of Thomas Jefferson University. Mice at 10 weeks of age were used for myocardial infarction (MI) experiments in which left anterior descending (LAD) coronary artery ligation was performed as described previously (Gao et al., 2010). After 30 minutes of MI, the slipknot was released, and the myocardium was reperfused.

Telemetry electrocardiographic (ECG) recording in conscious mice

Electrocardiographic (ECG) recordings were made with a Data Sciences International radiotelemetry data acquisition system (Dataquest A.R.T. version 2.2, Data Sciences International, MN) as described previously (Gao et al., 2010). A total of 17 mice (5 WT, 10 KO, 2 sham) were anesthetized with 2% isofluorane and implanted with a telemetry transmitter (Physio Tel EA-F20) in the dorsal back cranial to the hind limbs before surgical induction of IR. The two biopotential leads of the transmitter were placed subcutaneously in the lead II configuration (negative lead positioned at the right shoulder and the positive lead positioned about 2 cm to the left of the xyphoid process and caudal to the rib cage). Mice were housed in individual cages with unrestricted access to standard chow and drinking water. ECG was monitored for 30 minutes MI and after reperfusion recorded for 5 minutes every 15 minutes for 7 days. ECG data were collected and analyzed using Physiostat ECG analysis program version 4.02 (Data Sciences International, MN). ECG signals were digitally filtered and manually analyzed to detect arrhythmia identified by RR intervals two times greater or smaller than the mean, and quantified for 24 consecutive hours after induction of ischemia. Various functional parameters, including PVC, VT, RR interval, QRS duration, corrected QT interval and ST interval, were calculated.

Statistics

Data are expressed as mean ± s.e.m. Comparisons between groups were performed with a two-tailed Student *t* test using Microsoft Excel software. Statistical comparisons of between-group differences in ECG parameters were tested by two-way ANOVA. $P<0.05$ was considered statistically significant.

Acknowledgements

We thank Tino Hochepied, Craig Riley, David Kurz, Leeanne Griffith, Andrew Ho, Petra D'Hooge, and Paco Hulpiau for expert assistance, and the Bioimaging Facility of the Jefferson Kimmel Cancer Center for use of the confocal microscope.

Funding

This work was supported by the Jefferson Kimmel Cancer Center [NIH Cancer Center Core grant number 5 P30 CA-56036]; American Heart Association Scientist Development [grant number N2080068 to J.L.]; National Institutes of Health [grant number HL081569 to G.R.]; the Research Foundation – Flanders (FWO) [grant number G.0104.09N to F.v.R.]; and the Concerted Research Actions – Ghent University (GOA) [grant number 01G01908 to F.v.R.]. S.G. is a postdoctoral fellow with the FWO, and K.T. is a predoctoral fellow with the Flemish Agency for Innovation by Science and Technology (IWT). Deposited in PMC for release after 12 months.

Supplementary material available online at
http://jcs.biologists.org/lookup/suppl/doi:10.1242/jcs.098640/-/DC1

References

Basso, C., Corrado, D., Marcus, F. I., Nava, A. and Thiene, G. (2009). Arrhythmogenic right ventricular cardiomyopathy. *Lancet* **373**, 1289-1300.

Bauce, B., Nava, A., Beffagna, G., Basso, C., Lorenzon, A., Smaniotto, G., De Bortoli, M., Rigato, I., Mazzotti, E., Steriotis, A. et al. (2010). Multiple mutations in desmosomal proteins encoding genes in arrhythmogenic right ventricular cardiomyopathy/dysplasia. *Heart Rhythm* **7**, 22-29.

Borrmann, C. M., Grund, C., Kuhn, C., Hofmann, I., Pieperhoff, S. and Franke, W. W. (2006). The area composita of adhering junctions connecting heart muscle cells of vertebrates. II. Colocalizations of desmosomal and fascia adhaerens molecules in the intercalated disk. *Eur. J. Cell Biol.* **85**, 469-485.

Buchholz, F., Ringrose, L., Angrand, P. O., Rossi, F. and Stewart, A. F. (1996). Different thermostabilities of FLP and Cre recombinases: implications for applied site-specific recombination. *Nucleic Acids Res.* **24**, 4256-4262.

Cheng, L., Yung, A., Covarrubias, M. and Radice, G. L. (2011). Cortactin is required for N-cadherin regulation of Kv1.5 channel function. *J. Biol. Chem.* **286**, 20478-20489.

Chopra, N. and Knollmann, B. C. (2011). Gauging the risk of arrhythmic death by common genetic variants: resurgence of the sinister QT. *Circ. Cardiovasc. Genet.* **4**, 221-222.

Dekker, L. R., Fiolet, J. W., VanBavel, E., Coronel, R., Opthof, T., Spaan, J. A. and Janse, M. J. (1996). Intracellular Ca2+, intercellular electrical coupling, and mechanical activity in ischemic rabbit papillary muscle. Effects of preconditioning and metabolic blockade. *Circ. Res.* **79**, 237-246.

Delmar, M. and McKenna, W. J. (2010). The cardiac desmosome and arrhythmogenic cardiomyopathies: from gene to disease. *Circ. Res.* **107**, 700-714.

den Haan, A. D., Tan, B. Y., Zikusoka, M. N., Llado, L. I., Jain, R., Daly, A., Tichnell, C., James, C., Amat-Alarcon, N., Abraham, T. et al. (2009). Comprehensive desmosome mutation analysis in north americans with arrhythmogenic right ventricular dysplasia/cardiomyopathy. *Circ. Cardiovasc. Genet.* **2**, 428-435.

Drees, F., Pokutta, S., Yamada, S., Nelson, W. J. and Weis, W. I. (2005). Alpha-catenin is a molecular switch that binds E-cadherin-beta-catenin and regulates actin-filament assembly. *Cell* **123**, 903-915.

Franke, W. W., Borrmann, C. M., Grund, C. and Pieperhoff, S. (2006). The area composita of adhering junctions connecting heart muscle cells of vertebrates. I. Molecular definition in intercalated disks of cardiomyocytes by immunoelectron microscopy of desmosomal proteins. *Eur. J. Cell Biol.* **85**, 69-82.

French, A. P., Mills, S., Swarup, R., Bennett, M. J. and Pridmore, T. P. (2008). Colocalization of fluorescent markers in confocal microscope images of plant cells. *Nat. Protoc.* **3**, 619-628.

Gao, E., Lei, Y. H., Shang, X., Huang, Z. M., Zuo, L., Boucher, M., Fan, Q., Chuprun, J. K., Ma, X. L. and Koch, W. J. (2010). A novel and efficient model of coronary artery ligation and myocardial infarction in the mouse. *Circ. Res.* **107**, 1445-1453.

Gerull, B., Heuser, A., Wichter, T., Paul, M., Basson, C. T., McDermott, D. A., Lerman, B. B., Markowitz, S. M., Ellinor, P. T., MacRae, C. A. et al. (2004). Mutations in the desmosomal protein plakophilin-2 are common in arrhythmogenic right ventricular cardiomyopathy. *Nat. Genet.* **36**, 1162-1164.

Goossens, S., Janssens, B., Bonne, S., De Rycke, R., Braet, F., van Hengel, J. and van Roy, F. (2007). A unique and specific interaction between alphaT-catenin and plakophilin-2 in the area composita, the mixed-type junctional structure of cardiac intercalated discs. *J. Cell Sci.* **120**, 2126-2136.

Grossmann, K. S., Grund, C., Huelsken, J., Behrend, M., Erdmann, B., Franke, W. W. and Birchmeier, W. (2004). Requirement of plakophilin 2 for heart morphogenesis and cardiac junction formation. *J. Cell Biol.* **167**, 149-160.

Hirano, S., Kimoto, N., Shimoyama, Y., Hirohashi, S. and Takeichi, M. (1992). Identification of a neural alpha-catenin as a key regulator of cadherin function and multicellular organization. *Cell* **70**, 293-301.

Janssens, B., Goossens, S., Staes, K., Gilbert, B., van Hengel, J., Colpaert, C., Bruyneel, E., Mareel, M. and van Roy, F. (2001). alphaT-catenin: a novel tissue-specific beta-catenin-binding protein mediating strong cell-cell adhesion. *J. Cell Sci.* **114**, 3177-3188.

Janssens, B., Mohapatra, B., Vatta, M., Goossens, S., Vanpoucke, G., Kools, P., Montoye, T., van Hengel, J., Bowles, N. E., van Roy, F. et al. (2003). Assessment of the CTNNA3 gene encoding human alpha T-catenin regarding its involvement in dilated cardiomyopathy. *Hum. Genet.* **112**, 227-236.

Kostetskii, I., Li, J., Xiong, Y., Zhou, R., Ferrari, V. A., Patel, V. V., Molkentin, J. D. and Radice, G. L. (2005). Induced deletion of the N-cadherin gene in the heart leads to dissolution of the intercalated disc structure. *Circ. Res.* **96**, 346-354.

Lerner, D. L., Yamada, K. A., Schuessler, R. B. and Saffitz, J. E. (2000). Accelerated onset and increased incidence of ventricular arrhythmias induced by ischemia in Cx43-deficient mice. *Circulation* **101**, 547-552.

Li, J., Patel, V. V., Kostetskii, I., Xiong, Y., Chu, A. F., Jacobson, J. T., Yu, C., Morley, G. E., Molkentin, J. D. and Radice, G. L. (2005). Cardiac-specific loss of N-cadherin leads to alteration in connexins with conduction slowing and arrhythmogenesis. *Circ. Res.* **97**, 474-481.

Li, J., Levin, M. D., Xiong, Y., Petrenko, N., Patel, V. V. and Radice, G. L. (2008). N-cadherin haploinsufficiency affects cardiac gap junctions and arrhythmic susceptibility. *J. Mol. Cell. Cardiol.* **44**, 597-606.

Li, M. W., Mruk, D. D., Lee, W. M. and Cheng, C. Y. (2009). Connexin 43 and plakophilin-2 as a protein complex that regulates blood-testis barrier dynamics. *Proc. Natl. Acad. Sci. USA* **106**, 10213-10218.

Maass, K., Shibayama, J., Chase, S. E., Willecke, K. and Delmar, M. (2007). C-terminal truncation of connexin43 changes number, size, and localization of cardiac gap junction plaques. *Circ. Res.* **101**, 1283-1291.

Massey, K. D., Minnich, B. N. and Burt, J. M. (1992). Arachidonic acid and lipoxygenase metabolites uncouple neonatal rat cardiac myocyte pairs. *Am. J. Physiol.* **263**, C494-C501.

Oxford, E. M., Musa, H., Maass, K., Coombs, W., Taffet, S. M. and Delmar, M. (2007). Connexin43 remodeling caused by inhibition of plakophilin-2 expression in cardiac cells. *Circ. Res.* **101**, 703-711.

Pieperhoff, S. and Franke, W. W. (2007). The area composita of adhering junctions connecting heart muscle cells of vertebrates – IV: coalescence and amalgamation of desmosomal and adhaerens junction components – late processes in mammalian heart development. *Eur. J. Cell Biol.* **86**, 377-391.

Pieperhoff, S. and Franke, W. W. (2008). The area composita of adhering junctions connecting heart muscle cells of vertebrates. VI. Different precursor structures in non-mammalian species. *Eur. J. Cell Biol.* **87**, 413-430.

Pieperhoff, S., Schumacher, H. and Franke, W. W. (2008). The area composita of adhering junctions connecting heart muscle cells of vertebrates. V. The importance of plakophilin-2 demonstrated by small interference RNA-mediated knockdown in cultured rat cardiomyocytes. *Eur. J. Cell Biol.* **87**, 399-411.

Pogwizd, S. M. and Corr, P. B. (1987). Electrophysiologic mechanisms underlying arrhythmias due to reperfusion of ischemic myocardium. *Circulation* **76**, 404-426.

Saffitz, J. E. (2006). Adhesion molecules: why they are important to the electrophysiologist. *J. Cardiovasc. Electrophysiol.* **17**, 225-229.

Saffitz, J. E. (2009). Arrhythmogenic cardiomyopathy and abnormalities of cell-to-cell coupling. *Heart Rhythm* **6**, S62-S65.

Sato, P. Y., Musa, H., Coombs, W., Guerrero-Serna, G., Patino, G. A., Taffet, S. M., Isom, L. L. and Delmar, M. (2009). Loss of plakophilin-2 expression leads to decreased sodium current and slower conduction velocity in cultured cardiac myocytes. *Circ. Res.* **105**, 523-526.

Sato, P. Y., Coombs, W., Lin, X., Nekrasova, O., Green, K. J., Isom, L. L., Taffet, S. M. and Delmar, M. (2011). Interactions between ankyrin-g, plakophilin-2, and connexin43 at the cardiac intercalated disc. *Circ. Res.* **109**, 193-201.

Schoonjans, L., Kreemers, V., Danloy, S., Moreadith, R. W., Laroche, Y. and Collen, D. (2003). Improved generation of germline-competent embryonic stem cell lines from inbred mouse strains. *Stem Cells* **21**, 90-97.

Schwenk, F., Baron, U. and Rajewsky, K. (1995). A cre-transgenic mouse strain for the ubiquitous deletion of loxP-flanked gene segments including deletion in germ cells. *Nucleic Acids Res.* **23**, 5080-5081.

Scott, J. A. and Yap, A. S. (2006). Cinderella no longer: alpha-catenin steps out of cadherin's shadow. *J. Cell Sci.* **119**, 4599-4605.

Sen-Chowdhry, S., Morgan, R. D., Chambers, J. C. and McKenna, W. J. (2010). Arrhythmogenic cardiomyopathy: etiology, diagnosis, and treatment. *Annu. Rev. Med.* **61**, 233-253.

Sheikh, F., Chen, Y., Liang, X., Hirschy, A., Stenbit, A. E., Gu, Y., Dalton, N. D., Yajima, T., Lu, Y., Knowlton, K. U. et al. (2006). alpha-E-catenin inactivation disrupts the cardiomyocyte adherens junction, resulting in cardiomyopathy and susceptibility to wall rupture. *Circulation* **114**, 1046-1055.

Sohal, D. S., Nghiem, M., Crackower, M. A., Witt, S. A., Kimball, T. R., Tymitz, K. M., Penninger, J. M. and Molkentin, J. D. (2001). Temporally regulated and tissue-specific gene manipulations in the adult and embryonic heart using a tamoxifen-inducible Cre protein. *Circ. Res.* **89**, 20-25.

Torres, M., Stoykova, A., Huber, O., Chowdhury, K., Bonaldo, P., Mansouri, A., Butz, S., Kemler, R. and Gruss, P. (1997). An alpha-E-catenin gene trap mutation defines its function in preimplantation development. *Proc. Natl. Acad. Sci. USA* **94**, 901-906.

van Tintelen, J. P., Entius, M. M., Bhuiyan, Z. A., Jongbloed, R., Wiesfeld, A. C., Wilde, A. A., van der Smagt, J., Boven, L. G., Mannens, M. M., van Langen, I. M. et al. (2006). Plakophilin-2 mutations are the major determinant of familial arrhythmogenic right ventricular dysplasia/cardiomyopathy. *Circulation* **113**, 1650-1658.

Vanpoucke, G., Goossens, S., De Craene, B., Gilbert, B., van Roy, F. and Berx, G. (2004). GATA-4 and MEF2C transcription factors control the tissue-specific expression of the alphaT-catenin gene CTNNA3. *Nucleic Acids Res.* **32**, 4155-4165.

Xu, T., Yang, Z., Vatta, M., Rampazzo, A., Beffagna, G., Pilichou, K., Scherer, S. E., Saffitz, J., Kravitz, J., Zareba, W. et al. (2010). Compound and digenic heterozygosity contributes to arrhythmogenic right ventricular cardiomyopathy. *J. Am. Coll. Cardiol.* **55**, 587-597.

Yamada, S., Pokutta, S., Drees, F., Weis, W. I. and Nelson, W. J. (2005). Deconstructing the cadherin-catenin-actin complex. *Cell* **123**, 889-901.

Yan, G. X. and Kleber, A. G. (1992). Changes in extracellular and intracellular pH in ischemic rabbit papillary muscle. *Circ. Res.* **71**, 460-470.

Zhao, Z. M., Reynolds, A. B. and Gaucher, E. A. (2011). The evolutionary history of the catenin gene family during metazoan evolution. *BMC Evol. Biol.* **11**, 198.